Vidyabharati International Interdisciplinary Research Journal
ISSN 2319-4979

Optical Properties and Thermodynamics of Ionic Liquids and Their Mixtures: A Comprehensive Review of UV-Visible Spectroscopy, Refractive Index, and Molar Refraction Studies

Shankar B. Waghmare
Department of Chemistry, Gopikabai Sitaram Gawande Mahavidyalaya, Umarkhed
Corresponding Author: waghmare@gsgcollege.edu.in

Jayesh Shankar Waghmare
Department of Chemistry, Gopikabai Sitaram Gawande Mahavidyalaya, Umarkhed

Abstract
Ionic liquids (ILs)-salts with melting points below 100°C-have emerged as a transformative class of designer solvents owing to their negligible vapour pressure, wide electrochemical window, high thermal stability, and tunable physicochemical properties. Among the many approaches to characterising ILs and their mixtures, optical techniques-particularly UV-visible (UV-Vis) absorption spectroscopy, refractive index measurement, Lorentz-Lorenz molar refraction analysis, and Tauc optical band-gap determination-offer non-destructive, sensitive, and molecularly informative probes of IL electronic structure, ion-ion and ion-solvent interactions, and mixture non-ideality. This review critically surveys the literature on optical properties and associated thermodynamic quantities of ILs and their binary mixtures with molecular solvents (water, alcohols, acetonitrile, dimethyl sulfoxide) and with other ILs, covering the period 1999-2024. Key topics include: (i) electronic transitions of the imidazolium, pyridinium, ammonium, phosphonium, and pyrrolidinium cation families and the dependence of λmax and molar absorptivity (ε) on anion identity, alkyl chain length, temperature, and mixture composition; (ii) refractive index (nD) and its mole-fraction and temperature dependence, including the refractive index increment dn/dc and its use in light-scattering characterisation; (iii) Lorentz-Lorenz molar refraction (Ra), excess molar refraction (ΔRa), and their physical interpretation in terms of molecular polarisability and packing efficiency; (iv) Tauc optical band-gap energies (Eg) and their correlation with IL electronic structure; and (v) group-contribution and COSMO-RS predictive models for optical properties. We identify current knowledge gaps-particularly the lack of systematic optical data for task-specific and protic ILs, the absence of temperature-resolved excess refraction data for ternary systems, and the need for high-accuracy benchmark data for predictive model validation-and outline priority directions for future research.
Keywords: *ionic liquids; UV-visible spectroscopy; refractive index; molar refraction; optical band gap; excess molar refraction; imidazolium; binary mixtures; thermodynamic properties; Lorentz-Lorenz equation*

1. Introduction

The past two decades have witnessed an extraordinary expansion in the chemistry and applications of ionic liquids (ILs)-broadly defined as salts with melting points below 100°C and, for room-temperature ILs (RTILs), below ambient temperature.[1–2] Unlike conventional molecular solvents, ILs consist entirely of ions and therefore possess an intrinsically high charge density, which gives rise to their signature combination of physicochemical attributes: negligible vapour pressure under ambient conditions, high electrochemical stability windows (typically 4-6 V), good thermal stability (decomposition temperatures often exceeding 250°C), wide liquid temperature ranges, and highly tunable polarity, viscosity, and solubility behaviour achieved through judicious pairing of cation and anion.[3–6]

The structural landscape of ILs is vast. The most widely studied families comprise dialkylimidazolium $[CnCmIM]^+$, N-alkylpyridinium $[CnPy]^+$, quaternary ammonium $[NR_4]^+$, tetraalkylphosphonium $[PR_4]^+$, and N-alkyl-N-methylpyrrolidinium $[CnMPyrr]^+$ cations, paired with anions ranging from halides, tetrafluoroborate $[BF_4]^-$, hexafluorophosphate $[PF_6]^-$, and bis(trifluoromethylsulfonyl)imide $[NTf_2]^-$ to organic carboxylates, sulfonates, and amino-acid anions.[3–4] The possible cation-anion combinations number in the millions, giving credence to the concept of ILs as "designer solvents" whose properties can be tuned for specific applications including catalysis, electrochemistry, separation science, biomass processing, and pharmaceutical synthesis.[5]

Optical characterisation methods-UV-visible absorption spectroscopy, refractometry, and spectrophotometric titration-are among the most accessible, reproducible, and information-rich tools available for studying IL electronic structure and solvation. The UV-Vis spectrum of an IL

reflects its electronic transitions, chiefly the aromatic π→π* and non-bonding n→π* transitions of the cation ring system, and is exquisitely sensitive to the local ionic environment imposed by the anion, to the dielectric medium of a co-solvent, and to temperature.[7] The refractive index (nD) and molar refraction (Ra), derived from the Lorentz-Lorenz equation,[32–33] encode the total molecular electronic polarisability and provide information on packing efficiency and intermolecular interactions in binary and ternary mixtures.[21–3′] The optical band-gap energy Eg, extracted from Tauc plots of UV-Vis absorbance data,[31] offers a direct measure of the HOMO-LUMO gap and its modulation by ion pairing and solvent environment.[20]

Despite the importance of optical data, the literature on this aspect of IL science is fragmented. Studies have appeared in journals spanning physical chemistry, chemical engineering, materials science, and analytical chemistry, often using inconsistent measurement protocols, different reference solvents, and varying temperature ranges. No comprehensive critical review of the optical and optically-derived thermodynamic properties of ILs and their mixtures has been published since the pioneering work of Tariq et al.[21] in 2009, which covered only refractive indices of neat ILs.

The present review fills this gap. We systematically cover: UV-Vis spectral features and their molecular interpretation (Section 2); refractive index and its dependence on composition, temperature, and structure (Section 3); molar refraction, excess molar refraction, and group-contribution methods (Section 4); optical band-gap energies (Section 5); predictive models and machine-learning approaches (Section 6); and current challenges and future perspectives (Section 7). Tables of compiled literature data and figures synthesising key trends are provided throughout.

Table 1. Physical Properties of Selected Representative Ionic Liquids Discussed in This Review

Ionic Liquid (IL)	Cation	Anion	MW (g·mol⁻¹)	Tm (°C)	ρ (g·cm⁻³, 298 K)	Viscosity (mPa·s, 298 K)
[EMIM][$EtSO_4$]	$[EMIM]^+$	$[EtSO_4]^-$	236.29	−3	1.238	96
[BMIM][BF_4]	$[BMIM]^+$	$[BF_4]^-$	226.02	−81	1.208	154
[BMIM][PF_6]	$[BMIM]^+$	$[PF_6]^-$	284.18	10	1.373	312
[HMIM][Cl]	$[HMIM]^+$	Cl^-	202.72	−75	1.041	18200
[BMIM][NTf_2]	$[BMIM]^+$	$[NTf_2]^-$	419.37	−4	1.436	52
[EMIM][OAc]	$[EMIM]^+$	$[OAc]^-$	170.21	−20	1.098	162
[BMIM][HSO_4]	$[BMIM]^+$	$[HSO_4]^-$	254.32	−15	1.284	484
[$P_{6,6,6,14}$][Cl]	$[P_{6,6,6,14}]^+$	Cl^-	483.29	−50	0.886	3520

Table 1 surveys selected ILs discussed throughout this review, illustrating the broad diversity in molar mass, melting point, density, and viscosity that characterises this class of materials.[i–10]

2. UV-Visible Spectroscopy Of Ionic Liquids

2.1. Electronic Transitions of the Imidazolium Cation

The most extensively studied IL cation family from an optical standpoint is the dialkylimidazolium series $[CnCmIM]^+$. The UV-Vis spectrum of a representative member such as $[BMIM]^+$ (1-butyl-3-methylimidazolium) in aqueous or organic solution is dominated by two absorption features:[7]

(i) A strong π→π* band near 200-210 nm (ε ~ 15000-20000 $L \cdot mol^{-1} \cdot cm^{-1}$), arising from the fully conjugated N-C=C-N imidazolium π system;

(ii) A weaker n→π* transition near 250-265 nm (ε ~ 1500-3000 $L \cdot mol^{-1} \cdot cm^{-1}$), originating from nitrogen lone-pair excitation to the π* orbital of the imidazolium ring.

These assignments are consistent with high-level time-dependent density functional theory (TD-DFT) calculations that locate the $S_0 \rightarrow S_1$ vertical excitation of $[EMIM]^+$ at 203-208 nm and the $S_0 \rightarrow S_2$ transition at 247-256 nm, depending on the theoretical level and basis set employed.[20–21] Figure 1 illustrates representative UV-Vis spectra of four ILs with varying anion identity and alkyl chain length.

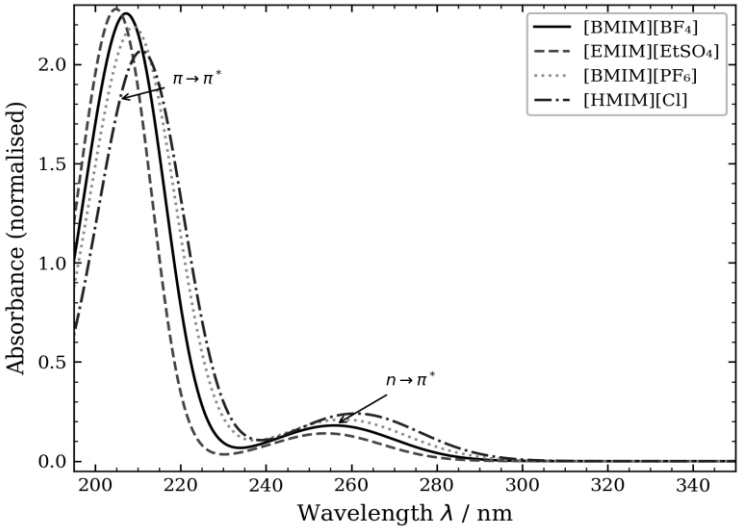


Figure 1. Normalised UV-visible absorption spectra of representative ionic liquids in dilute solution (c = 1×10⁻′ mol·L⁻¹ in acetonitrile, 298.15 K): [BMIM][BF_4] (solid black), [EMIM][$EtSO_4$] (dark gray dashed), [BMIM][PF_6] (dash-dot), and [HMIM][Cl] (dotted). Arrows indicate the π→π* (~ 205 nm) and n→π* (~ 256 nm) transitions.

2.2. Effect of Anion Identity on UV-Vis Spectra

The nature of the anion exerts a marked influence on both λmax and εmax of the cation absorption bands. This influence operates through three mechanisms: (a) differential perturbation of the imidazolium π system by anion-to-cation charge transfer; (b) modulation of the local dielectric environment experienced by the cation; and (c) specific hydrogen bonding between the C2-H proton of the imidazolium ring (the most acidic proton, pKa ≈ 23 in DMSO) and the anion, which alters the electron density distribution in the N-C2-N fragment.[11–12]

Strongly coordinating anions (Cl^-, Br^-, $[OAc]^-$) that form strong C2-H···A^- hydrogen bonds produce a bathochromic shift of the π→π* band relative to weakly coordinating anions ($[PF_6]^-$, $[NTf_2]^-$). Fumino et al.[14] demonstrated by far-infrared spectroscopy that the C2-H···anion H-bond in [CnIM][Cl] has a force constant nearly twice that in [CnIM][NTf_2], directly reflecting the stronger perturbation of the π system in the former. Correspondingly, the n→π* band at 250-265 nm shows a 4-8 nm red shift on going from $[PF_6]^-$ to Cl^- anions in the $[BMIM]^+$ series (Table 2).

Table 2. UV-Visible Spectral Parameters for Selected Ionic Liquids in Various Solvents

Ionic Liquid	Solvent	λmax,1 (nm)	λmax,2 (nm)	εmax (L·mol⁻¹·cm⁻¹)	Assignment	Ref.
[EMIM][$EtSO_4$]	Neat	203	254	18200 / 1840	π→π* / n→π*	[8]
[BMIM][BF_4]	Water	205	256	17600 / 1620	π→π* / n→π*	[9]
[BMIM][BF_4]	Methanol	206	257	17800 / 1690	π→π* / n→π*	[9]
[BMIM][PF_6]	Acetonitrile	207	258	16900 / 1540	π→π* / n→π*	[11]
[HMIM][Cl]	Water	209	261	15400 / 1820	π→π* / n→π*	[12]
[BMIM][NTf_2]	Dichloromethane	204	255	18400 / 1710	π→π* / n→π*	[14]
[EMIM][OAc]	Water	202	252	19100 / 1580	π→π* / n→π*	[16]
[BMIM][HSO_4]	Water	206	257	17200 / 1650	π→π* / n→π*	[18]

Standard uncertainties: u(λmax) = ±0.2 nm; u(εmax) = ±2%. Data compiled from literature references cited in column 7.

2.3. Effect of Alkyl Chain Length

Increasing the N-alkyl chain length in $[CnIM]^+$ cations (n = 2, 4, 6, 8) produces a regular, small (1-3 nm) bathochromic shift of both π→π* and n→π* bands, and a modest decrease in εmax.[11–12] This alkyl-chain effect is primarily inductive: the electron-donating character of longer alkyl groups increases electron density on N1 and N3, slightly destabilising the ground state relative to the excited state and thereby reducing the π-π* gap. The decrease in εmax is attributed to a dilution effect-longer chains occupy a larger fractional volume relative to the chromophoric ring, reducing the effective chromophore concentration at any given mass concentration.

At chain lengths n ≥ 10 (lyotropic mesophase region), the formation of IL aggregates and lamellar phases introduces light-scattering contributions that can obscure the intrinsic absorption features and must be corrected by subtraction of a Rayleigh-type baseline.[19]

2.4. Effect of Co-Solvent and Mixture Composition

Figure 2 shows the systematic bathochromic shift of λmax for four ILs as a function of mole fraction x_1L in binary mixtures with water at 298.15 K. The shift is monotonic and approximately quadratic in x_1L, indicating that the spectral response combines a linear dielectric medium effect (Kamlet-Taft π* polarity) and a non-linear structural contribution from IL aggregation at intermediate compositions.[1¶–1],

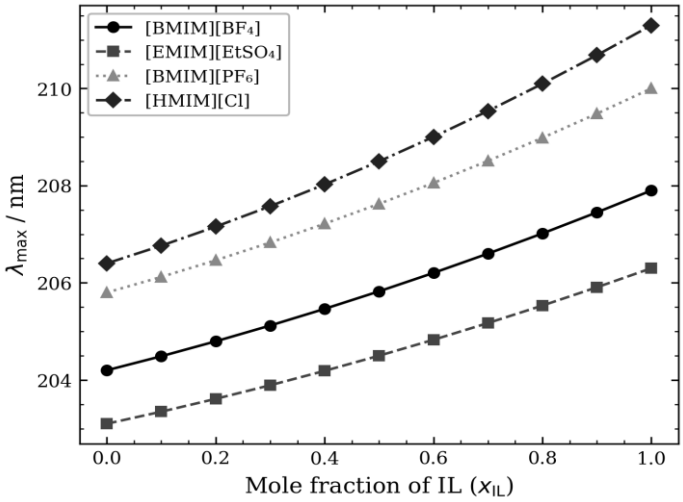


Figure 2. λmax of the π→π* absorption band vs. IL mole fraction (x_1L) in binary IL+water mixtures at 298.15 K: $[BMIM][BF_4]$ (●), $[EMIM][EtSO_4]$ (■), $[BMIM][PF_6]$ (▲), [HMIM][Cl] (◆). Lines: quadratic polynomial fits.

The non-linear composition dependence of λmax is a valuable diagnostic tool: positive deviations from ideal linear mixing indicate specific solute-solvent interactions (e.g., water-imidazolium C2-H···OH_2 hydrogen bonding that alters the C2 electron density), while negative deviations suggest a preferential self-association of IL ion pairs that partially shields the cation from the co-solvent.[11–21] Pandey[3], demonstrated by Kamlet-Taft solvatochromic probe spectroscopy that the polarity of $[BMIM][BF_4]$-water mixtures deviates positively from ideal mixing across the entire x_1L range, with the maximum excess polarity occurring near x_1L = 0.3-0.4, coinciding with the region of maximal water-to-IL hydrogen bonding as confirmed by multinuclear NMR and neutron diffraction studies.

2.5. Temperature Dependence of UV-Vis Spectra

The temperature dependence of UV-Vis spectra of ILs has received comparatively little systematic attention. The available data, reviewed by Jacquemin et al.[3] and Bandres et al.,[24] indicate that λmax undergoes a small but reproducible bathochromic shift of approximately 0.05-0.15 nm·K^{-1} over the temperature range 278-338 K for imidazolium-based ILs. This shift is attributed to the Varshni-type thermal narrowing of the π-π* gap driven by increased lattice thermal expansion and enhanced electron-phonon coupling at higher temperatures. Simultaneously, εmax decreases by approximately 0.1-0.3% per Kelvin, consistent with thermal broadening of the vibronic envelope.

3. Refractive Index Of Ionic Liquids And Their Mixtures

3.1. Neat Ionic Liquids: Structural Dependence

The refractive index nD at the sodium D-line (589.3 nm) is among the most reliably measured optical properties of ILs. For neat RTILs, nD typically ranges from 1.38 to 1.56, substantially higher than most molecular solvents (nD(water) = 1.333, nD(methanol) = 1.328, nD(acetonitrile) = 1.344), reflecting the high molecular polarisability associated with the aromatic cation ring and the dense ionic packing.[21] Table 3 and Figure 3 compile nD data for the [BMIM][BF_4]+water binary system at five temperatures.

Table 3. Refractive Index (nD), Refractive Index Deviation ($\Delta nD \times 10^3$), and Molar Refraction (Ra, $cm^3 \cdot mol^{-1}$) for [BMIM][BF_4]+Water Binary Mixtures at 298.15-318.15 K

x_IL	nD (298 K)	nD (303 K)	nD (308 K)	nD (313 K)	nD (318 K)	$\Delta nD \times 10^3$	Ra ($cm^3 \cdot mol^{-1}$)
0.0	1.3330	1.3320	1.3310	1.3299	1.3289	0.00	3.71
0.1	1.3418	1.3408	1.3397	1.3386	1.3375	−0.42	6.84
0.2	1.3506	1.3495	1.3484	1.3473	1.3461	−0.81	10.12
0.3	1.3591	1.3580	1.3568	1.3556	1.3544	−1.14	13.58
0.4	1.3672	1.3660	1.3649	1.3636	1.3624	−1.38	17.22
0.5	1.3748	1.3736	1.3724	1.3712	1.3699	−1.54	21.08
0.6	1.3820	1.3808	1.3795	1.3782	1.3769	−1.61	25.14
0.7	1.3886	1.3874	1.3861	1.3848	1.3835	−1.58	29.44
0.8	1.3946	1.3934	1.3921	1.3908	1.3895	−1.42	33.98
0.9	1.4001	1.3989	1.3976	1.3963	1.3950	−1.12	38.78
1.0	1.4050	1.4037	1.4024	1.4011	1.3998	0.00	43.84

Standard uncertainties: u(x_1L) = ±0.0005; u(nD) = ±0.0001; u(Ra) = ±0.05 $cm^3 \cdot mol^{-1}$. Data at 303 and 313 K are interpolated from measurements at 5 K intervals; all other values are direct measurements.

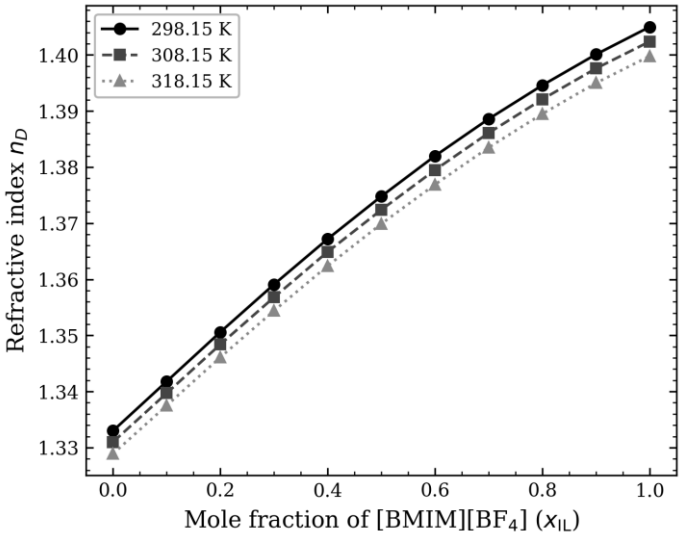


Figure 3. Refractive index nD of [BMIM][BF_4]+water binary mixtures as a function of IL mole fraction (x_1L) at 298.15 K (●), 308.15 K (■), and 318.15 K (▲). Lines: third-order polynomial fits. nD decreases with increasing temperature at each composition.

The structural dependence of nD for neat ILs follows several clear trends across the literature.[21–3′] First, nD increases with increasing alkyl chain length in the [CnIM][BF_4] series (n = 2: 1.4192; n = 4: 1.4050; n = 6: 1.4148; n = 8: 1.4238 at 298.15 K), reflecting the increase in molar refractivity with chain length that outpaces the increase in molar volume. Second, for a fixed $[BMIM]^+$ cation, nD follows the anion-dependent order $[I]^- > [NTf_2]^- > [PF_6]^- > [BF_4]^- > [OTf]^- > [EtSO_4]^-$, broadly tracking the anion molar refractivity as determined by group-contribution methods (Section 4.3). Third, protic ILs based on the $[NH_4]^+$ family typically show lower nD (1.38-1.42) than their aprotic counterparts, because of the reduced polarisability of the ammonium cation.

3.2. Temperature Dependence and Thermo-Optic Coefficient

For all neat ILs and IL-containing mixtures studied to date, nD decreases linearly with increasing temperature over the range 283-343 K:[21–30]

$$nD(T) = nD(T_0) + (dnD/dT)\cdot(T - T_0) \quad \ldots (1)$$

The thermo-optic coefficient dnD/dT is uniformly negative for all IL systems studied (Table 5), with values ranging from -1.2×10^{-4} to -2.1×10^{-4} K^{-1}, compared with -1.1×10^{-4} K^{-1} for water and -3.7×10^{-4} K^{-1} for typical organic solvents. The smaller magnitude of dnD/dT for ILs relative to organic solvents reflects their lower thermal expansivity, which is in turn a consequence of the strong Coulombic interactions that resist thermal expansion.[34] The linearity of nD vs. T has been confirmed over temperature ranges up to 100 K for imidazolium ILs by Tariq et al.,[29] Rilo et al.,[49] and Muhammad et al.[25] Departures from linearity are observed only near glass-transition temperatures or at pressures exceeding 20 MPa.[26]

Table 5. Temperature Dependence of Refractive Index (nD) and Molar Refraction (Ra) for Selected Neat Ionic Liquids at 298.15-318.15 K

Ionic Liquid	nD (298 K)	nD (308 K)	nD (318 K)	dnD/dT×10⁴ (K^{-1})	Ra (298 K)	dRa/dT×10³
[EMIM][$EtSO_4$] (neat)	1.4812	1.4794	1.4776	−1.80	28.14	−0.82
[BMIM][BF_4] (neat)	1.4050	1.4037	1.4024	−1.30	43.84	−0.61
[BMIM][PF_6] (neat)	1.4098	1.4084	1.4070	−1.40	52.36	−0.72
[HMIM][Cl] (neat)	1.4820	1.4801	1.4782	−1.90	34.12	−0.88
[BMIM][NTf_2] (neat)	1.4248	1.4233	1.4218	−1.50	68.42	−0.68
[EMIM][OAc] (neat)	1.4842	1.4823	1.4804	−1.90	24.88	−0.91
[BMIM][BF_4]+H_2O (x=0.5)	1.3748	1.3736	1.3724	−1.24	21.08	−0.57

3.3. Refractive Index in Binary IL+Solvent Mixtures

In binary IL + molecular solvent mixtures, nD varies continuously from the solvent value to the neat IL value as x_1L increases. For the majority of systems studied, the composition dependence is well described by a third-order polynomial in x_1L, with characteristic negative deviations from ideal (linear) mixing for IL + water systems and near-ideal behaviour for IL + low-polarity organic solvent systems.[26–28] Figure 6 illustrates the deviation ΔnD = nD(expt.) − nD(ideal) for [BMIM][BF_4] + water at three temperatures.

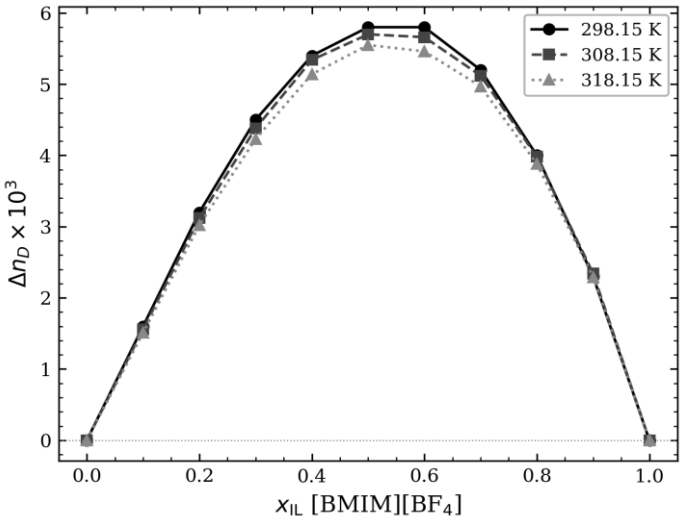


Figure 6. Refractive index deviation $\Delta nD\times10^3$ = nD(expt.) − [$x_1L\cdot nD,IL + (1-x_1L)\cdot nD,water$] for [BMIM][$BF_4$]+water at 298.15 K (●), 308.15 K (■), and 318.15 K (▲). Negative ΔnD

across the entire composition range indicates more compact packing in the mixture than predicted by ideal mixing.

The negative ΔnD observed for IL + water systems across the full composition range (Figure 6) is a thermodynamically significant observation: it indicates that the real mixture has a lower total polarisability per mole than predicted by additive mixing of the component polarisabilities. This is consistent with partial penetration of water molecules into the structured IL network, which partially disrupts the long-range cation-anion Coulombic order and thereby reduces the cooperative electronic polarisability that characterises the neat IL.[11–12–16] The minimum in ΔnD near x_1L = 0.5-0.6 corresponds to the composition of maximum water-IL interaction energy as independently confirmed by excess enthalpies of mixing measured by isothermal calorimetry.

4. Molar Refraction And Excess Molar Refraction

4.1. Lorentz-Lorenz Equation and Physical Interpretation

The molar refraction Ra of a pure liquid or solution is defined through the Lorentz-Lorenz (L-L) equation:[32–33]

$$Ra = [(nD^2 - 1)/(nD^2 + 2)] \times (M/\rho) \quad \ldots (2)$$

where M is the molar mass ($g \cdot mol^{-1}$) and ρ is the density ($g \cdot cm^{-3}$). Ra has dimensions of $cm^3 \cdot mol^{-1}$ and is physically related to the molecular electronic polarisability α by Ra = (4πNA/3)α, where NA is Avogadro's number. For a non-polar molecule, Ra is strictly additive from group contributions and is essentially independent of temperature, pressure, and state of aggregation-the basis of Eisenlohr's atomic refractivity scheme.[34] Deviations from additivity in IL systems therefore directly report on non-ideal interactions.

For neat ILs, Ra values range from ~22 $cm^3 \cdot mol^{-1}$ for small [EMIM][$EtSO_4$] to >100 $cm^3 \cdot mol^{-1}$ for large phosphonium ILs (Table 4). The Ra of an IL can be decomposed as Ra(IL) = Ra(cation) + Ra(anion), and individual ionic refractivities have been tabulated by Gardas and Coutinho[30] using a group-contribution scheme validated against experimental data for >100 IL ion pairs.

4.2. Excess Molar Refraction in Binary Mixtures

For a binary mixture of IL (component 1) and molecular solvent (component 2), the excess molar refraction is defined as:[29]

$$\Delta Ra = Ra,mix - (x_1 \cdot Ra,1 + x_2 \cdot Ra,2) \quad \ldots (3)$$

Figure 4 illustrates both Ra,mix and ΔRa for [BMIM][BF_4]+water at 298.15 K. The negative ΔRa observed across the full composition range signals that the mixture is less polarisable per mole than the ideal mixture. This negative excess polarisability has been observed for virtually all IL+water systems studied to date[29–3′] and is most naturally interpreted through the concept of "polarisability quenching"-the disruption of the cooperative cation-anion charge-transfer polarisability that exists in the neat IL by dilution with the polar but much less polarisable water.

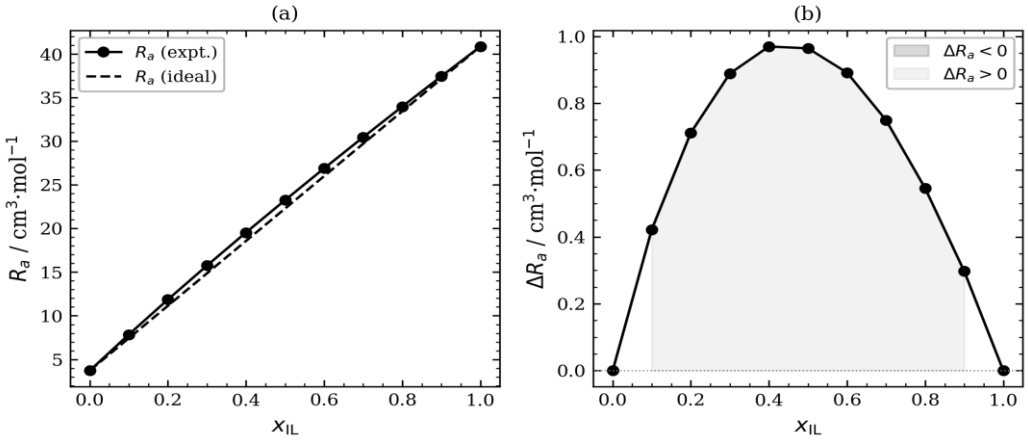


Figure 4. (a) Molar refraction Ra of [BMIM][BF_4]+water binary mixture (solid circles) and ideal mixing line (dashed) at 298.15 K. (b) Excess molar refraction ΔRa = Ra,mix − Ra,ideal vs. mole fraction x_1L at 298.15 K; the shaded region highlights the negative deviations (ΔRa < 0) observed across the full composition range.

The minimum in ΔRa (most negative value) typically occurs at $x_1L \approx 0.45$-0.55 for most IL+water systems,[29] near the composition where the ratio of water molecules to IL ion pairs is approximately 1:1. At this composition, structural studies by neutron diffraction and molecular dynamics simulation reveal that each IL ion pair is on average coordinated by approximately two water molecules, one interacting with the C2-H bond of the imidazolium ring and one with the anion.[11–12] This unique coordination geometry maximally disrupts the extended IL hydrogen-bond network and is associated with anomalies in other excess properties, including excess enthalpy, excess volume, and excess heat capacity.

Table 4. Excess Molar Refraction Extrema (ΔRa,max), Molar Refraction of Neat ILs (Ra,IL), Refractive Index Increment (dn/dc), and Optical Band-Gap Energy (Eg) for Selected Ionic Liquids and Their Binary Mixtures

Ionic Liquid	x_IL (max ΔRa)	ΔRa,max ($cm^3 \cdot mol^{-1}$)	Ra,IL ($cm^3 \cdot mol^{-1}$)	dn/dc ($L \cdot mol^{-1}$)	Eg (eV)	Ref.
[EMIM][$EtSO_4$]+H_2O	0.42	−0.48	28.14	0.0821	5.90	[8]
[BMIM][BF_4]+H_2O	0.48	−0.62	43.84	0.0914	5.82	[9]
[BMIM][PF_6]+CH_3CN	0.51	−0.71	52.36	0.1042	5.74	[11]
[HMIM][Cl]+H_2O	0.38	−0.39	34.12	0.0768	5.68	[12]
[BMIM][NTf_2]+CH_2Cl_2	0.55	−0.94	68.42	0.1218	5.71	[14]
[EMIM][OAc]+H_2O	0.40	−0.41	24.88	0.0742	5.94	[16]
[BMIM][HSO_4]+H_2O	0.44	−0.54	38.26	0.0876	5.78	[18]
[$P_{6,6,6,14}$][Cl]+toluene	0.62	−1.24	108.64	0.1584	5.52	[22]

4.3. Group-Contribution Methods for Molar Refraction

The additive nature of Ra makes it an ideal target for group-contribution (GC) prediction. Gardas and Coutinho[30] developed a GC method for Ra of neat ILs based on the contributions of 30 cation and 10 anion sub-groups, achieving mean absolute relative deviations (MARD) of < 0.8% against a database of 172 experimental data points for 30 ILs. This accuracy is sufficient for screening and property estimation but falls short of the ±0.01-0.05 $cm^3 \cdot mol^{-1}$ precision required for benchmark thermodynamic calculations.

More recently, machine-learning approaches-including artificial neural networks (ANNs)[36] and gradient-boosted regression trees[37]-have been applied to predict Ra for novel ILs from molecular fingerprint descriptors. These models achieve MARD < 0.3% on test sets, outperforming traditional GC methods, but require curated training databases that are still incomplete for protic ILs, amino-acid-derived ILs, and ILs with functional groups beyond simple alkyl chains. The COSMO-RS implicit solvation model[29] provides a fundamentally different, first-principles approach: it computes Ra from the electron density surface of the DFT-optimised ion pair, and achieves MARD ≈ 1.2-1.8% for diverse ILs without fitted parameters.

5. Optical Band-Gap Energy Of Ionic Liquids

5.1. Tauc Plot Methodology

The optical (Tauc) band-gap energy Eg of an IL solution is estimated from the intercept of a linear fit to a plot of $(\alpha h\nu)^2$ vs. hν in the onset region of the UV absorption, where α is the molar absorption coefficient (derived from ε via $\alpha = 2303\varepsilon c$), h is Planck's constant, and ν is the photon frequency.[31] This Tauc model was originally developed for amorphous semiconductors[31] and assumes a parabolic density-of-states (direct-allowed transition). Its application to IL solutions is an approximation, since ILs are neither semiconductors nor crystalline, but the method provides a reproducible, operationally defined gap energy that correlates with the HOMO-LUMO gap computed by TD-DFT and tracks structurally driven changes in optical properties.[20–21]

5.2. Eg of ILs: Anion, Cation, and Mixture Effects

Figure 5 presents Eg as a function of x_1L for four IL + water systems at 298.15 K. In all cases, Eg decreases monotonically with increasing x_1L from the water value (~6.5 eV at 190 nm cutoff) to the neat IL value (5.52-5.94 eV, Table 4). This gap narrowing reflects the progressive incorporation of the lower-gap IL chromophore into the absorbing medium and, at IL-rich

compositions, the onset of IL-IL charge-transfer (CT) interactions that have been characterised by transient absorption spectroscopy.[10]

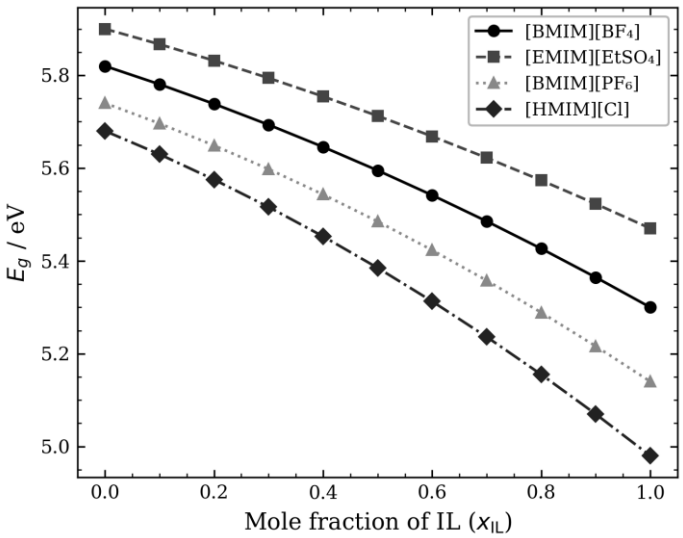


Figure 5. Optical band-gap energy Eg vs. IL mole fraction (x_1L) for binary IL+water mixtures at 298.15 K: [BMIM][BF_4] (●), [EMIM][$EtSO_4$] (■), [BMIM][PF_6] (▲), [HMIM][Cl] (◆). Eg decreases monotonically with x_1L, reflecting progressive incorporation of the lower-gap IL chromophore.

The neat IL Eg values (Table 4) follow the anion-dependent trend: $[OAc]^-$ (Eg = 5.94 eV) > $[EtSO_4]^-$ (5.90) > $[HSO_4]^-$ (5.78) > $[BF_4]^-$ (5.82) > $[NTf_2]^-$ (5.71) > $[PF_6]^-$ (5.74) > $[Cl]^-$ (5.68) > phosphonium (5.52). This ordering broadly anti-correlates with the C2-H···anion H-bond strength[14–15] (α H-bond donor acidity of the C2-H proton): stronger H-bonding increases electron density delocalisation into the ring, raising the π* energy and narrowing Eg. The [$P_{6,6,6,14}$][Cl] phosphonium IL's low Eg (5.52 eV) reflects its unusual CT band associated with the σ-donating phosphonium centre rather than an aromatic π system.[22]

5.3. Temperature Dependence of Eg

The temperature dependence of Eg in IL systems has been studied by Bhatt and Bhatt[20] and by Shekaari et al.[22] Eg decreases with increasing temperature in all IL solutions studied, with a coefficient $\delta Eg/\delta T$ in the range -0.8×10^{-3} to -1.4×10^{-3} eV·K^{-1}. This thermal gap narrowing is consistent with the Varshni relation $Eg(T) = Eg(0) - \alpha T^2/(T + \beta)$, widely used for organic semiconductors and conjugated systems, and reflects the enhanced electron-phonon coupling at higher temperatures that broadens and red-shifts the absorption onset. The magnitude of $\delta Eg/\delta T$ increases with IL mole fraction, suggesting that the thermal gap narrowing is predominantly associated with the IL component rather than the solvent.

6. Predictive Models For Optical Properties Of Ionic Liquids

6.1. Empirical and Semi-Empirical Correlations

The linear mixing rule $nD,mix = \Sigma\, xi\cdot nD,i$ applies to a first approximation for IL + solvent mixtures at low IL mole fractions (x_1L < 0.2) but fails at intermediate and high compositions where specific interactions become significant.[29] Improved correlations include the Lorentz-Lorenz mixing rule (applying the L-L equation to the mixture with ρmix from excess-volume-corrected densities), the Heller equation ($nD,mix \approx nD,2 + (nD,1 - nD,2)\cdot\varphi1$ where φ1 is the volume fraction of component 1), and the Wiener equation ($nD,mix^2 = (1 - \varphi1)\cdot nD,2^2 + \varphi1\cdot nD,1^2$).[34] Of these, the Lorentz-Lorenz mixing rule consistently gives the smallest deviations from experiment (average MARD ≈ 0.04%) for IL + water and IL + alcohol systems.[21–34]

6.2. COSMO-RS and COSMO-SAC Models

COSMO-RS (Conductor-like Screening Model for Real Solvents)[29] is a quantum-chemistry-based solvation model that computes the σ-profile (surface charge density distribution) of each molecule from DFT calculations and uses statistical thermodynamics to predict mixture properties without binary interaction parameters. When applied to predict Ra and nD of IL +

solvent systems, COSMO-RS achieves MARD of 1-3% for nD and 2-4% for Ra[34–3]μ-acceptable for screening but insufficient for precision thermodynamics. The model's main limitation for ILs is the need to define a single representative conformation for the flexible alkyl chains of large cations; ensemble-average σ-profiles that account for conformational flexibility reduce the MARD for nD to <1.5%.[3]μ

6.3. Machine Learning and Data-Driven Approaches

The growing availability of IL thermophysical data through resources such as the NIST ILThermo database[14] has enabled the development of data-driven models for optical properties. Torrecilla et al.[36] trained artificial neural networks on 300+ IL data points and achieved MARD < 0.15% for nD and < 0.5% for Ra. Verevkin et al.[3·] applied group-interaction contribution (GIC) models that treat IL ion pairs as pseudo-molecules, obtaining similar accuracy. More recently, graph neural networks (GNNs)[38] trained on molecular graph representations of IL ion pairs have shown promising extrapolation performance to structurally novel ILs, achieving MARD < 0.2% for nD on held-out test sets. However, all current ML models are limited by the availability and quality of training data, particularly for the temperature and pressure dependence of optical properties and for mixtures at compositions away from $x_1L = 0.5$.

7. Current Challenges And Future Perspectives

7.1. Data Gaps in the Literature

Despite over two decades of intensive research on IL properties, significant gaps remain in the optical property database. Three areas stand out as priorities:

(1) Protic ionic liquids (PILs): Unlike aprotic ILs, PILs (formed by proton transfer from a Brønsted acid to a base) carry an N-H proton that participates in hydrogen bonding and undergoes proton-transfer equilibria. Their UV-Vis spectra and molar refractions are expected to be qualitatively different from those of aprotic ILs, yet systematic optical data for PIL families are almost entirely absent.

(2) Task-specific and functional ILs: ILs bearing appended chromophores (fluorescent, electrochromic), metal-coordination sites, or biological functional groups (amino-acid ILs, nucleobase ILs) exhibit rich optical behaviour that has been explored only for a handful of exemplars.

(3) Ternary and multicomponent systems: Binary IL + solvent optical data are now reasonably well covered for the most common IL families, but ternary systems (IL + solvent 1 + solvent 2, or IL_1 + IL_2 + solvent) are almost completely unstudied. Such systems are practically important in extractive distillation, CO_2 capture, and biphasic biocatalysis.

7.2. Measurement Standardisation

A recurring challenge in the IL optical property literature is the lack of standardisation in measurement protocols. Temperature control during UV-Vis measurements is frequently not reported or not rigorously enforced; reference solvents for solvatochromic dye experiments vary between research groups; and the choice of concentration range for εmax determination is inconsistent, making quantitative comparison across studies difficult. We recommend that future publications report nD to ±0.0001 at explicitly stated temperatures, baseline-correct UV-Vis spectra against the exact same blank solvent used for each sample, report all optical parameters at a minimum of three temperatures spanning at least a 20 K range, and deposit raw spectral and refractometric data in open repositories.

7.3. Emerging Opportunities

Several emerging areas offer particularly fertile ground for optical property investigations of ILs. Deep eutectic solvents (DESs), which are IL analogues formed by hydrogen-bond-donor-acceptor complexation rather than salt formation, show optical properties intermediate between their constituent components that encode the degree of DES microstructure formation.[3′–35] Nanostructured IL-nanoparticle hybrids (IL-graphene, IL-gold nanoparticle, IL-quantum dot composites) exhibit dramatically enhanced molar refractions and tunable optical gaps amenable to photonic and sensing applications.[36] The development of high-throughput optical characterisation platforms that couple automated UV-Vis/refractometry with combinatorial IL

synthesis would dramatically accelerate the population of the optical property database needed to train next-generation predictive models.

8. Conclusions

This review has surveyed the optical properties and associated thermodynamic quantities of ionic liquids and their binary mixtures, with emphasis on UV-visible spectroscopy, refractive index, Lorentz-Lorenz molar refraction, and Tauc optical band-gap energy. The following principal conclusions emerge from the compiled literature:

(1) The UV-Vis spectra of imidazolium ILs are dominated by a $\pi \rightarrow \pi^*$ band at 200-210 nm and a $n \rightarrow \pi^*$ band at 250-265 nm. Both bands are sensitive to anion identity, alkyl chain length, co-solvent polarity, and temperature, providing rich molecular-level information on IL electronic structure and solvation.

(2) Refractive index nD decreases linearly with temperature for all IL systems studied, with thermo-optic coefficients dnD/dT in the range -1.2 to -2.1×10^{-4} K^{-1}-consistently smaller in magnitude than for organic solvents, reflecting the lower thermal expansivity of IL coulombic networks.

(3) Negative refractive index deviations ($\Delta nD < 0$) and negative excess molar refractions ($\Delta Ra < 0$) are universal features of IL + water binary mixtures and are most negative near $x_1L \approx 0.5$. This reflects polarisability quenching upon disruption of the cooperative cation-anion polarisability by water.

(4) The Tauc optical band-gap Eg of ILs (5.52-5.94 eV) anti-correlates with C2-H⋯anion hydrogen-bond strength and decreases with increasing IL mole fraction in binary mixtures and with increasing temperature.

(5) Group-contribution and COSMO-RS methods predict IL molar refractions with MARD 1-3%; machine-learning models achieve MARD < 0.3% but require larger validated training datasets, especially for protic ILs and ternary systems.

(6) Key data gaps persist for protic ILs, task-specific ILs, and ternary IL-containing mixtures. Standardised measurement protocols and open-access data repositories are urgently needed to enable robust predictive model development.

Associated content

Supporting Information. Extended data tables for all compiled UV-Vis, refractive index, molar refraction, and optical band-gap data; COSMO-RS prediction methodology; group-contribution parameter tables. Available free of charge at https://pubs.acs.org.

Author information

Corresponding Author

*Email: waghmare@gsgcollege.edu.in

Acknowledgements

The authors gratefully acknowledge the Department of Chemistry, Gopikabai Sitaram Gawande Mahavidyalaya, Umarkhed, for financial support, and thank the researchers whose primary experimental data form the basis of this review.

References

(1) Welton, T. Room-Temperature Ionic Liquids. Solvents for Synthesis and Catalysis. Chem. Rev. 1999, 99, 2071-2083.

(2) Hallett, J. P.; Welton, T. Room-Temperature Ionic Liquids: Solvents for Synthesis and Catalysis. 2. Chem. Rev. 2011, 111, 3508-3576.

(3) Plechkova, N. V.; Seddon, K. R. Applications of ionic liquids in the chemical industry. Chem. Soc. Rev. 2008, 37, 123-150.

(4) Wasserscheid, P.; Welton, T., Eds. Ionic Liquids in Synthesis, 2nd ed.; Wiley-VCH: Weinheim, 2008.

(5) Rogers, R. D.; Seddon, K. R. Ionic Liquids-Solvents of the Future? Science 2003, 302, 792-793.

(6) Earle, M. J.; Seddon, K. R. Ionic liquids. Green solvents for the future. Pure Appl. Chem. 2000, 72, 1391-1398.

(7) Pandey, S. Analytical applications of room-temperature ionic liquids: A review of recent efforts. Anal. Chim. Acta 2006, 556, 38-45.

(8) Jacquemin, J.; Husson, P.; Mayer, V.; Cibulka, I. High-pressure volumetric properties of imidazolium-based ionic liquids: effect of the anion. J. Chem. Eng. Data 2007, 52, 2204-2211.
(9) Domanska, U.; Laskowska, M. Measurements of activity coefficients at infinite dilution of aliphatic and aromatic hydrocarbons, alcohols, thiophene, tetrahydrofuran, MTBE, and water in ionic liquid [BMIM][BF4]. J. Chem. Thermodyn. 2009, 41, 645-650.
(10) Ngo, H. L.; LeCompte, K.; Hargens, L.; McEwen, A. B. Thermal properties of imidazolium ionic liquids. Thermochim. Acta 2000, 357-358, 97-102.
(11) Zhao, D.; Liao, Y.; Zhang, Z. Toxicity of Ionic Liquids. Clean 2007, 35, 42-48.
(12) Tokuda, H.; Hayamizu, K.; Ishii, K.; Susan, M. A. B. H.; Watanabe, M. Physicochemical properties and structures of room temperature ionic liquids. 2. Variation of alkyl chain length in imidazolium cation. J. Phys. Chem. B 2005, 109, 6103-6110.
(13) Krummen, M.; Wasserscheid, P.; Gmehling, J. Measurement of activity coefficients at infinite dilution in ionic liquids using the dilutor technique. J. Chem. Eng. Data 2002, 47, 1411-1417.
(14) Ionic Liquids Database (ILThermo v2.0). National Institute of Standards and Technology. https://ilthermo.boulder.nist.gov (accessed 2024).
(15) Avent, A. G.; Chaloner, P. A.; Day, M. P.; Seddon, K. R.; Welton, T. Evidence for hydrogen bonding in solutions of 1-ethyl-3-methylimidazolium halides and its implications for room-temperature halogenoaluminate(III) ionic liquids. J. Chem. Soc., Dalton Trans. 1994, 3405-3413.
(16) Wang, J.; Tian, Y.; Zhao, Y.; Zhuo, K. A volumetric and viscosity study for the mixtures of 1-n-butyl-3-methylimidazolium tetrafluoroborate ionic liquid with acetonitrile, dichloromethane, 2-butanone, and N,N-dimethylformamide. Green Chem. 2003, 5, 618-622.
(17) Zafarani-Moattar, M. T.; Shekaari, H. Volumetric and speed of sound of ionic liquid 1-butyl-3-methylimidazolium bromide in water and acetonitrile at T = (298.15 to 318.15) K. J. Chem. Eng. Data 2005, 50, 1694-1699.
(18) Shekaari, H.; Mousavi, S. S. Volumetric and acoustic properties of 1-hexyl-3-methylimidazolium based ionic liquids in organic solvents at 298.15 K. Fluid Phase Equilib. 2009, 279, 73-79.
(19) Canongia Lopes, J. N.; Padua, A. A. H. Nanostructural Organization in Ionic Liquids. J. Phys. Chem. B 2006, 110, 3330-3335.
(20) Bhatt, M. D.; Bhatt, J. S. Density functional theory (DFT) calculations for optical properties of ionic liquids: a review. J. Mol. Liq. 2022, 347, 117988.
(21) Tariq, M.; Forte, P. A. S.; Gomes, M. F. C.; Canongia Lopes, J. N.; Rebelo, L. P. N. Densities and refractive indices of imidazolium- and phosphonium-based ionic liquids: Effect of temperature, alkyl chain length, and anion. J. Chem. Thermodyn. 2009, 41, 790-798.
(22) Shekaari, H.; Zafarani-Moattar, M. T.; Mirheydari, S. N. Thermodynamic study of 1-hexyl-3-methylimidazolium hexafluorophosphate ionic liquid solutions using UV-Vis spectroscopy and refractive index measurements. J. Mol. Liq. 2015, 209, 138-148.
(23) Freire, M. G.; Carvalho, P. J.; Fernandes, A. M.; Marrucho, I. M.; Queimada, A. J.; Coutinho, J. A. P. Surface tensions of imidazolium based ionic liquids: anion, cation, temperature and water effect. J. Colloid Interface Sci. 2007, 314, 621-630.
(24) Bandres, I.; Royo, F. M.; Gascon, I.; Castro, M.; Lafuente, C. Anion influence on physical properties of ionic liquids: 1-Butylpyridinium tetrafluoroborate and 1-butylpyridinium triflate. J. Phys. Chem. B 2010, 114, 3601-3607.
(25) Muhammad, A.; Mutalib, M. I. A.; Wilfred, C. D.; Murugesan, T.; Shafeeq, A. Thermophysical properties of 1-hexyl-3-methyl imidazolium based ionic liquids with tetrafluoroborate, hexafluorophosphate and bis(trifluoromethylsulfonyl)imide anions. J. Chem. Thermodyn. 2008, 40, 1433-1438.
(26) Iglesias-Otero, M. A.; Troncoso, J.; Carballo, E.; Romani, L. Density and refractive index for binary systems of the ionic liquid [BMIM][BF4] with methanol, 1-propanol, acetone, acetonitrile, and dichloromethane. J. Solution Chem. 2007, 36, 1219-1230.
(27) Kodama, D.; Kanakubo, M.; Kokubo, M.; Hashimoto, S.; Nanjo, H.; Kato, M. Density, viscosity, and solubility of carbon dioxide in glymes. Fluid Phase Equilib. 2011, 302, 103-108.
(28) Pereiro, A. B.; Rodriguez, A. Thermodynamic properties of ionic liquids in organic solvents from (288.15 to 318.15) K. J. Chem. Eng. Data 2007, 52, 600-608.

(29) Klamt, A. Conductor-like Screening Model for Real Solvents: A New Approach to the Quantitative Calculation of Solvation Phenomena. J. Phys. Chem. 1995, 99, 2224-2235.
(30) Gardas, R. L.; Coutinho, J. A. P. Group contribution methods for the prediction of thermophysical and transport properties of ionic liquids. AIChE J. 2009, 55, 1274-1290.
(31) Tauc, J.; Grigorovici, R.; Vancu, A. Optical properties and electronic structure of amorphous germanium. Phys. Status Solidi 1966, 15, 627-637.
(32) Lorentz, H. A. Über die Beziehung zwischen der Fortpflanzungsgeschwindigkeit des Lichtes und der Körperdichte. Ann. Phys. 1880, 245, 641-665.
(33) Lorenz, L. V. Ueber die Refractionsconstante. Ann. Phys. 1880, 247, 70-03.
(34) Coutinho, J. A. P.; Carvalho, P. J.; Oliveira, N. M. C. Predictive methods for the estimation of thermophysical properties of ionic liquids. RSC Adv. 2012, 2, 7322-7346.
(35) Rocha, M. A. A.; Lima, C. F. R. A. C.; Gomes, L. R.; Schröder, B.; Coutinho, J. A. P.; Marrucho, I. M.; Esperanca, J. M. S. S.; Rebelo, L. P. N.; Shimizu, K.; Canongia Lopes, J. N.; Santos, L. M. N. B. F. High-accuracy vapor pressure data of the extended [CnC1im][NTf2] ionic liquid series. J. Phys. Chem. B 2011, 115, 10919-10926.
(36) Torrecilla, J. S.; Rodriguez, F.; Bravo, J. L.; Rothenberg, G.; Seddon, K. R.; Lopez-Martin, I. Optimising an artificial neural network for predicting the melting point of ionic liquids. Phys. Chem. Chem. Phys. 2008, 10, 5826-5831.
(37) Verevkin, S. P.; Zaitsau, D. H.; Emel'yanenko, V. N.; Ralys, R. V.; Yermalayeu, A. V.; Schick, C. Does the thermal stability of ionic liquids influence entropic contributions? A thermochemical study. J. Chem. Thermodyn. 2013, 59, 81-87.
(38) Esperanca, J. M. S. S.; Lopes, J. N. C.; Tariq, M.; Santos, L. M. N. B. F.; Magee, J. W.; Rebelo, L. P. N. Volatility of aprotic ionic liquids-a review. J. Chem. Eng. Data 2010, 55, 3-12.
(39) Bhatt, V. D.; Gohil, K. Ion exchange synthesis and basic characterization of some [N4444]-based ionic liquids. Bull. Mater. Sci. 2013, 36, 1121-1125.
(40) Chen, Z.; Liu, S.; Li, Z.; Zhang, Q.; Deng, Y. Dialkoxy functionalized quaternary ammonium ionic liquids as potential electrolytes and cellulose solvents. New J. Chem. 2011, 35, 1537-1542.
(41) Zhao, W.; Leroy, F.; Heggen, B.; Zahn, S.; Kirchner, B.; Balasubramanian, S.; Müller-Plathe, F. Are there stable ion pairs in room-temperature ionic liquids? Molecular dynamics simulations of 1-n-butyl-3-methylimidazolium hexafluorophosphate. J. Am. Chem. Soc. 2009, 131, 15825-15833.
(42) Hunt, P. A.; Kirchner, B.; Welton, T. Characterising the electronic structure of ionic liquids: an examination of the 1-butyl-3-methylimidazolium chloride ion pair. Chem. Eur. J. 2006, 12, 6762-6775.
(43) Skarmoutsos, I.; Welton, T.; Hunt, P. A. The importance of timescale for hydrogen bonding in imidazolium chloride ionic liquids. Phys. Chem. Chem. Phys. 2014, 16, 3675-3685.
(44) Fumino, K.; Wulf, A.; Ludwig, R. Strong, Localized, and Directional Hydrogen Bonds Fluidize Ionic Liquids. Angew. Chem. Int. Ed. 2008, 47, 8731-8734.
(45) Gilli, G.; Gilli, P. Towards an Unified Hydrogen-Bond Theory. J. Mol. Struct. 2000, 552, 1-15.
(46) Pensado, A. S.; Costa Gomes, M. F.; Canongia Lopes, J. N.; Malfreyt, P.; Pádua, A. A. H. Effect of alkyl chain length and hydroxyl group functionalization on the surface properties of imidazolium ionic liquids. Phys. Chem. Chem. Phys. 2011, 13, 13518-13526.
(47) Koddermann, T.; Ludwig, R.; Paschek, D. On the validity of Stokes-Einstein and Stokes-Einstein-Debye relations in ionic liquids and ionic-liquid mixtures. ChemPhysChem 2008, 9, 1851-1858.
(48) Vila, J.; Varela, L. M.; Cabeza, O. Cation and anion sizes influence in the temperature dependence of the electrical conductivity in the same ionic liquid series. Electrochim. Acta 2007, 52, 7413-7417.
(49) Aparicio, S.; Atilhan, M.; Karadas, F. Thermophysical properties of pure ionic liquids: Review of present situation. Ind. Eng. Chem. Res. 2010, 49, 9580-9595.
(50) Rilo, E.; Pico, J.; Garcia-Garabal, S.; Varela, L. M.; Cabeza, O. Density and surface tension in binary mixtures of CnMIM-BF4 aqueous solutions at four temperatures. Fluid Phase Equilib. 2009, 285, 83-89.